

REGULARIZATION PHASE AND AUXILIARY POTENTIAL TO MAINTAIN ADIABATIC QUANTUM DYNAMICS AT DELTA FUNCTION POTENTIAL

Siti Rohayati ^{1*}, Iwan Setiawan ², Eko Risdianto ³

^{1,2,3} Physics Education Study Program, Bengkulu University, Bengkulu 38122, Indonesia
E-mail: ^{1*} sitiroyayati1812@gmail.com; ² iwansetiawan@unib.ac.id; ³ eko_risdianto@unib.ac.id

* Corresponding Author

Abstract

This study aims to determine the wave function solution in quantum systems with delta function potential, regularization phase (θ), additional potential (\tilde{V}) and current density (J) to maintain adiabatic quantum dynamics. This research was conducted by reviewing the literature regarding efforts to maintain adiabatic quantum dynamics. The fast-forward method is applied to the delta function potential with scattered and bound conditions and then validated using Wolfram Mathematica software. Furthermore, the wave function solution is obtained in the form of an exponential graph, in the state $E < 0$ forms an exponential function graph uphill for $x < 0$ and downhill for $x > 0$ where when $x = 0$ m the wave function is equal to k , while the wave function in the state $E > 0$ forms an amplitude graph with a wavelength that is directly proportional to the value of k . The regularization phase at state $E < 0$ forms an exponential graph and never intersects the x -axis where at $x < 0$ when the value of $x = -1$ m, $\theta_1 = -4$ and when x is positive θ_1 is getting closer to zero while at $x > 0$ when $x = 1$, $\theta_2 = 4$ and at negative x the value of θ_2 is getting closer to zero. In the state of $E > 0$ the regularization phase forms a graph that opens up and down with an increase in the minimum value and a decrease in the maximum value that is constant for ($x < 0$). The additional potential is in the form of a parabolic graph where the $E > 0$ state forms a parabola for ($x < 0$) where when $x = 3$ m, the potential is 6×10^{-102} Volts and forms a constant graph for $x > 0$ with a value of 2.2×10^{-68} Volts, and forms a linear graph for ($x > 0$). The current meeting at the $E < 0$ state forms a descending exponential function graph for the reflected current meeting, where when $x = -1$ m the reflected current meeting is 0.5×10^{-33} A/m² and when x is positive the reflected current meeting is close to zero. The exponential graph rises for the passing current density where when $x = 1$ m the passing current density is 0.5×10^{-33} A/m², and when x is negative the passing current density is close to zero. In the state of ($E > 0$) the inrush and reflected current densities form a linear graph. In the incoming current density graph when $k = -1$ m⁻¹ the value of the incoming current density is 0, and when $k = 0$ m⁻¹ the value of the current density is 1×10^{-34} A/m². On the graph of the reflected current density when $k = 1$ the current density is 0, and when the current density is 1×10^{-34} A/m², k is 0 m. While the passing current density forms a parabolic graph where the minimum passing current density value is at $k = -1$ m and rises as the value of k increases.

Keywords: Adiabatic Quantum Dynamics, Phase Regularization, Fast-forward Method, Delta Function Potential, Auxiliary Potential

How to Cite: Siti Rohayati, S., Setiawan, I., Risdianto, E. (2023). C Regularization Phase and Auxiliary Potential to Maintain Adiabatic Quantum Dynamics at Delta Function Potential. *Jurnal Pendidikan Fisika dan Keilmuan (JPFK)*, 9(2), 87-113. doi: <http://doi.org/10.25273/jpfk.v9i2.18405>.

Introduction

One important factor in the process of producing a product such as electronics, automotive and plants is production time. Efficiency will be obtained if the time needed to produce a product is shorter. Efforts to speed up the microscopic world will be able to change the characteristics of these particles. However, efficiency is not obtained if the required time speed changes the physical characteristics and content of a particle (Ainayah et al., 2022: 1). To overcome this problem, a concept has been found to speed up a process to achieve equilibrium without changing the characteristics of particles called the adiabatic concept. The adiabatic concept can be achieved but for a long time. A suitable method was found to speed up the product manufacturing process without changing the characteristics of the system reviewed (Setiawan, 2019: 57).

A system can be reviewed in two viewpoints: macroscopic and microscopic. The microscopic view reviews a portion of the probability formed and influenced by arteries of similar properties (Novita et al., 2017: 189). Meanwhile, the macroscopic view can be viewed from the general nature of the system on a large scale as an example of thermodynamics (Viridi & Khotimah, 2010: 12). The system that we will review in an effort to shorten the process of making a product is a microscopic system.

In microscopic systems, in order to shorten the dynamical process, it is necessary to maintain the properties and characteristics of the system, which are called adiabatic states. Adiabatic quantum dynamics is a term for the concept of accelerating quantum dynamics by maintaining the characteristics of each energy level of the system (Elisa et al., 2022: 2). The adiabatic process is very important in manipulating particle dynamics because with this process a system does not experience changes in state before and after the dynamic process. The adiabatic process can be done but with a long time. So it is still less efficient when used to make a product. To solve this problem, a method is needed to accelerate adiabatic quantum dynamics. Some of the methods being developed are *fast forward* methods and *shortcuts to adiabaticity* (STA).

The *fast forward* method is a method used to speed up the time in making a product including fast film projection on the screen (Nakamura et al., 2017: 1). Nakamura and Masuda succeeded in developing a *fast forward* method on relativistic systems (Benggadinda & Setiawan, 2021: 275). Several studies have used the fast forward method, including the fast forward method in the multi-object system (Masuda & Nakamura, 2022), the fast forward method in the carnot machine, the *fast forward* method in tunneling (Khujakulov & Nakamura, 2016) (Nakamura et al., 2017: 1) and several other studies.

In addition, there is also another method of accelerating adiabatic dynamics called STA. The *shortcuts to adiabaticity* (STA) method was developed by scientists Gonzale Muga, Xi Chen and Del Campo. In this method, efforts to accelerate quantum dynamics can be done through quantum phase transitions (Del Campo, 2013: 1). In addition to achieving speed, the STA method also has important features, namely the many alternative routes that can be used as control parameters and flexibility to optimize relevant variables, including to minimize energy excitation and energy consumption (Guéry-Odelin et al., 2019: 2).

Talking about the microscopic world, there is a branch of physics that specifically studies the world, starting from its symptoms, characteristics and properties, the science is called quantum mechanics (Syaifudin et al., 2015: 1). Suparmi in (Dianawati et al., 2017: 1) explained that quantum mechanics also studies

the behavior of matter and its interaction with energy at the atomic to subatomic scales. In the quantum world, the behavior of particles can be described in terms of wave functions derived from solving the Schrödinger equation. The result of solving the Schrödinger equation can be an energy spectrum and a wave function that provides information about the behavior of particles affected by potential (Cari et al., 2012:113). One potential that can affect is the delta potential.

According to Griffiths (2005: 68) the delta dirac function is a very high and narrow spike at the origin point whose area is 1. Haberman in (Susanti et al., 2019: 693) states that the delta function was first discovered by Dirac in 1926, that is, a function that has a value of zero except at its source point and the integral along its domain interval is equal to one. In research conducted by (Susanti et al., 2019: 693) the delta function is used to show the location of a single electric charge located in a volume at its source point. Then the delta function is also used to model the non-homogeneous part of the electric potential difference equation that has been obtained in the form of the Poisson equation. In electrodynamics, the charge density of a point charge is a delta function. The delta function can be thought of as the limit of a series of functions, such as a rectangle or triangle whose height increases and width decreases.

Benggadinda and Setiawan (2021) reviewed the application of *fast forward* theory to accelerate adiabatic quantum dynamics on a single spin. In the study, the regularization term of the hamiltonian H and the driving magnetic field have been obtained which can accelerate the time needed to change the direction of spin, from the direction of $\uparrow_{up} \begin{pmatrix} 1 \\ 0 \end{pmatrix}$ at the beginning state ($t = 0$) to the down state $\downarrow \begin{pmatrix} 0 \\ 1 \end{pmatrix}$ at the final state. With the addition of the hamiltonian term and the driving magnetic field, this magnetic field is referred to as the driving magnetic field guarantees that a single spin can move from the z to $-z$ direction in a short time and move adiabatically while maintaining the energy state of the system at the *ground state*.

This study reviews electrons that will move from one state to another but are blocked by a barrier potential, namely the delta function potential. These electrons are expected to move with a fast time and fixed characteristics. The characteristics of an electron can be maintained using the adiabatic concept. The adiabatic concept can be done but with a very long time. So a *fast-forward* method is needed that is able to accelerate the adiabatic quantum dynamics.

In this study, the author applied *fast forward* to quantum systems with certain potentials. The potential reviewed is the potential of the delta function. Through this research will be determined the general solution of wave function, regularization phase (θ), additional potential (\tilde{V}) and current density (J) to maintain adiabatic quantum dynamics at delta function potential.

Methods

This research is a research to examine quantitative physical theories by conducting literature studies related to adiabatic quantum theory and delta function potential. Literature study is one method of conducting research. In this method, research is carried out by reviewing and tracing the results of writing on previous researchers. The term literature study is also often referred to as literature study (Restu et al., 2021: 35).

This research was conducted from August to November at the Physics Education Study Program, Faculty of Teacher Training and Education, Bengkulu University. With the research procedure as described in Figure 1 below:

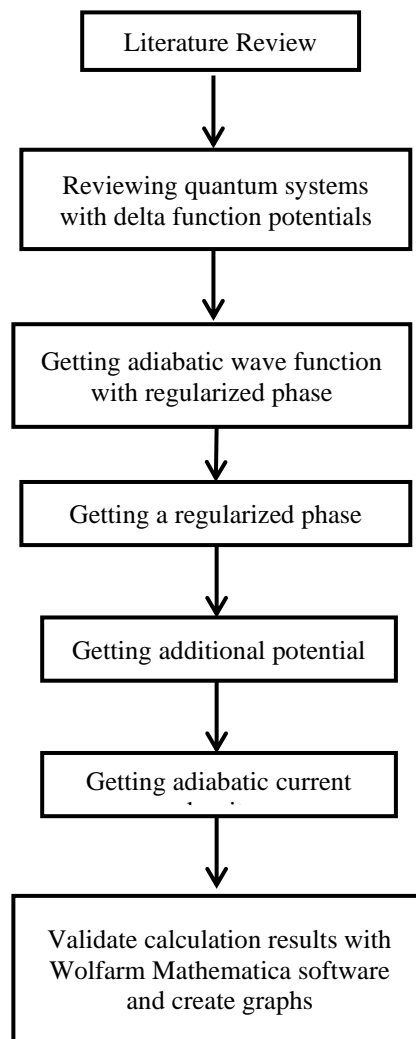


Figure 1. Research procedure chart

1. Literature review

At this stage the author prepares research by searching and collecting supporting literaturesuch as books, journals and other related references. In this study the quantum, Schrödinger equation, adiabatic quantum theorem, fast forward method, and delta function potential of earlier researchers.

2. Reviewing quantum systems with delta function potentials

This step is done by examining the existing Schrödinger equation, then entering the delta function potential into the Schrödinger equation until obtaining the general equation of the wave function in the delta function potential.

3. Getting adiabatic wave function with regularized phase

The general equation of the wave function that has previously been obtained, then searched for each of its constants. After obtaining the value of each constant, substitute it back into the delta potential wave function until a potential wave function of the delta function with a regularized phase is obtained.

4. Getting a regularized phase

At this stage, the regularized phase is sought by deriving the adiabatic Schrödinger equation until it can be separated from real and imaginary forms. The real part is then used to find the regularized phase.

5. Getting additional potential

The imaginary part of the derivative of the Adrialactic Schrödinger equation is used to find additional potential values.

6. Getting adiabatic current density

The adiabatic wave function from the delta function potential is then separated according to the type of current, inflow, reflected current and current through. After that, the current density is found using the current density formula.

7. Validate calculation results with Wolfram Mathematica software and create graphs

At this stage, the calculation results that have been obtained are validated by matching the *Wolfram Mathematica software*. After the calculation results are matched, an amplitude graph is created using the same *software*.

Sources that can be used in the study of literature are not original. Not all research writings can be used as references. Writings that are worth using include books by trusted authors, accredited scientific journals, and student research results in various forms such as theses, theses, dissertations and so on. In conducting literature studies, there are several methods such as *criticize, compare, summarize, and synthesize* (Restu et al., 2021: 35).

In this study, validation was carried out using *Mathematica software*. *Wolfram Mathematica* is a computing program by *Stephen Wolfram* founded in 1987. *Software* is able to complete many mathematical programs including algebra, integrals, matrices and graphs. According to Haswati and Nopitasari (2019: 8), *Mathematica* is a computer algebra system (CAS) that can integrate several computing capabilities including symbolic, numeric, visualization (graphics), programming languages and *word processing* into an easy-to-use environment. This *software* can support graphing of the completion of a linear program by inputting similarities and inequalities (Sunaryo 2020: 88). In addition to validating the calculation results, in this study graphing was also assisted by this *software*.

The method to be used is the *fast-forward* method to maintain adiabatic quantum dynamics with the potential of the delta function. According to Setiawan et al (2018: 1) the adiabatic quantum theorem states that if a system is in a momentary Hamiltonian eigenstate, then the system will remain so during the adiabatic process. The *fast-forward* method introduced by Masuda and Nakamura deals with the acceleration of quantum dynamics. This theory was developed to accelerate adiabatic quantum dynamics by introducing a large timescale factor in adiabatic dynamics guaranteed by regularization provisions (Setiawan et al. 2019: 1). *Fast-forward* theory guarantees the acceleration of certain quantum evolution and obtains the desired target state in a shorter time scale, by accelerating the dynamics of reference quantum (Setiawan, Gunara, and Nakamura, 2019: 1).

Results And Discussion

The potential of the delta function can be written as follows:

$$V(x) = -\alpha\delta(x) \quad (1)$$

Substitute equation (1) into the Schrödinger equation so that it becomes:

$$-\frac{\hbar^2}{2m} \frac{d^2\psi}{dx^2} - \alpha\delta(x)\psi = E\psi \quad (2)$$

with α is a positive constant.

In general, the solution to the wave function of the Schrodinger equation can be written as follows:

$$\Psi_n(x, t) = \psi_n(x)e^{-i\omega t} \quad (3)$$

With that in mind, $\omega = \frac{E}{\hbar}$ the equation can be rewritten (3) as follows:

$$\Psi_n(x, t) = \Psi_n(x, t)e^{-(i/\hbar) \int_0^t E_n dt} \Psi_n(x, t) = \Psi_n(x, t)e^{-(i/\hbar) \int_0^t E_n dt} \quad (4)$$

The parameter t is modified to be $R(t)$ with:

$$R(t) = R_0 + \varepsilon t \quad ; \varepsilon \ll 1 \quad (5)$$

with ε is an adiabatic parameter that causes the system to move slowly. By adding adiabatic phase (θ) and adiabatic parameters, (ε) the adiabatic wave function regularized to: (Masuda & Nakamura, 2010)

$$\begin{aligned} i\hbar \frac{\partial \Psi_n^{(reg)}}{\partial t} &= -\frac{\hbar^2}{2m} \frac{\partial^2 \Psi_n^{(reg)}}{\partial x^2} + V^{(reg)}(x, t) \Psi_n(x, R(t)) \\ i\hbar \frac{\partial \Psi_n^{(reg)}}{\partial t} &= -\frac{\hbar^2}{2m} \frac{\partial^2 \Psi_n^{(reg)}}{\partial x^2} + V^{(reg)}(x, t) \Psi_n(x, R(t)) \end{aligned} \quad (6)$$

with is $\Psi_n^{(reg)}$ an adiabatic wave function and $V^{(reg)}$ is a regularized potential. $V^{(reg)}$ obtained from regularized Hamiltonians when regularizing wave functions with

$$V^{(reg)}(x, t) = V_0(x, R(t)) + \varepsilon \tilde{V}(x, t). V^{(reg)} V^{(reg)} V^{(reg)}(x, t) = V_0(x, R(t)) + \varepsilon \tilde{V}(x, t).$$

Equations (6) are decreased and regularized so as to produce real and imaginary equations (more in (6)(Hutagalung et al., 2023: 7))

Real

$$\begin{aligned} |\psi_n|^2 \frac{\partial^2 \theta}{\partial x^2} + 2\text{Re} \left[\psi_n \frac{\partial \psi_n^*}{\partial x} \right] \frac{\partial \theta}{\partial x} + \frac{2m_0}{\hbar} \text{Re} \left[\psi_n \frac{\partial \psi_n^*}{\partial R} \right] &= 0 \quad |\psi_n|^2 \frac{\partial^2 \theta}{\partial x^2} + 2\text{Re} \left[\psi_n \frac{\partial \psi_n^*}{\partial x} \right] \frac{\partial \theta}{\partial x} + \\ \frac{2m_0}{\hbar} \text{Re} \left[\psi_n \frac{\partial \psi_n^*}{\partial R} \right] &= 0 \quad |\psi_n|^2 \frac{\partial^2 \theta}{\partial x^2} + 2\text{Re} \left[\psi_n \frac{\partial \psi_n^*}{\partial x} \right] \frac{\partial \theta}{\partial x} + \frac{2m_0}{\hbar} \text{Re} \left[\psi_n \frac{\partial \psi_n^*}{\partial R} \right] = 0 \end{aligned} \quad (7)$$

Imaginer

$$\begin{aligned} \frac{\hbar}{m_0} \text{Im} \left(\psi_n^* \frac{\partial \psi_n}{\partial x} \right) \frac{\partial \theta}{\partial x} + \frac{\tilde{V}}{\hbar} |\psi_n|^2 + \text{Im} \left[\psi_n^* \frac{\partial \psi_n}{\partial R} \right] + \frac{\partial \theta}{\partial t} |\psi_n|^2 &= 0 \quad \frac{\hbar}{m_0} \text{Im} \left(\psi_n^* \frac{\partial \psi_n}{\partial x} \right) \frac{\partial \theta}{\partial x} + \frac{\tilde{V}}{\hbar} |\psi_n|^2 + \\ \text{Im} \left[\psi_n^* \frac{\partial \psi_n}{\partial R} \right] + \frac{\partial \theta}{\partial t} |\psi_n|^2 &= 0 \end{aligned} \quad (8)$$

where \hbar is Planck's constant, ψ is a position-dependent wave function, θ is a \hbar regularized phase, \tilde{V} is an ψ auxiliary potential, $R(t)$ is a modified Parameter t , ε is an adiabatic parameter, Ψ is a θ position and time-dependent wave function, α is a positive constant, and $R(t) \Psi^* \varepsilon \Psi$ is a conjugate wave function.

The real part (equation (7)) is used to calculate the adiabatic phase (θ) and the imaginary part ((θ) equation (8)) is used to calculate the additional potential. (\tilde{V}) With reference to equation (7) if the wave function is a function real and does not

contain the variable R, then the part containing R is considered zero, so the equation becomes:

$$|\psi_n|^2 \frac{\partial^2 \theta}{\partial x^2} + 2 \operatorname{Re} \left[\psi_n \frac{\partial \psi_n^*}{\partial x} \right] \frac{\partial \theta}{\partial x} = 0 \quad (9)$$

integrate the two segments, so that the general equation of the adiabatic phase (θ) for wave functions that do not contain R and is real is as follows: (θ)

$$\theta_n = A_n \int \frac{1}{|\psi_n|^2} dx \quad (10)$$

As for calculating the general equation of the adiabatic phase (θ), if the wave function is an imaginary function and does not contain the variable R, (θ) the part containing the variable R and the real function is considered zero so that it becomes:

$$\theta_n = \frac{A_n x}{|\psi_n|^2} \quad (11)$$

The adiabatic potential (\tilde{V}) can be calculated using equation (8). If the wave function is a real function that does not contain R then the equation containing R and is imaginary is considered zero, equation (8) can be rewritten as follows:

$$\frac{\tilde{V}}{\hbar} |\psi_n|^2 = 0 \quad (12)$$

Based on equation (12) for a wave function that is a real function and does not contain R, the additional potential (\tilde{V}) is zero. (\tilde{V})

While the adiabatic potential (\tilde{V}) for wave functions that contain imaginary functions and do not contain R can be written as follows:

$$\tilde{V} = -\frac{\hbar}{m_0} \operatorname{Im} \left(\psi_n^* \frac{\partial \psi_n}{\partial x} \right) \frac{\partial \theta}{\partial x} \quad (13)$$

The density of adiabatic current (J) in general can be determined by the following formula:

$$j = \frac{i\hbar}{2m} \left(\Psi^{(reg)}(x, R(t)) \frac{d\Psi^{(reg)*}(x, R(t))}{dx} - \Psi^{(reg)*}(x, R(t)) \frac{d\Psi^{(reg)}(x, R(t))}{dx} \right) \quad (14)$$

The equation of the three types of current density can be written as follows: (J_{masuk}) (J_{pantul}) (J_{lewat})

$$J_{masuk} = \frac{i\hbar}{2m} \left(\Psi^{(reg)}(x, R(t))_{masuk} \frac{d\Psi^{(reg)*}(x, R(t))_{masuk}}{dx} - \Psi^{(reg)*}(x, R(t))_{masuk} \frac{d\Psi^{(reg)}(x, R(t))_{masuk}}{dx} \right) \quad (15)$$

$$J_{pantul} = \frac{i\hbar}{2m} \left(\Psi^{(reg)}(x, R(t))_{pantul} \frac{d\Psi^{(reg)*}(x, R(t))_{pantul}}{dx} - \Psi^{(reg)*}(x, R(t))_{pantul} \frac{d\Psi^{(reg)}(x, R(t))_{pantul}}{dx} \right) \quad (16)$$

$$J_{lewat} = \frac{i\hbar}{2m} \left(\Psi^{(reg)}(x, R(t))_{lewat} \frac{d\Psi^{(reg)*}(x, R(t))_{lewat}}{dx} - \Psi^{(reg)*}(x, R(t))_{lewat} \frac{d\Psi^{(reg)}(x, R(t))_{lewat}}{dx} \right) \quad (17)$$

The reflection coefficient (R) and transmission coefficient (T) can be calculated. (R) (T)

$$R = \frac{|J_{pantul}|}{|J_{masuk}|} \quad (18)$$

$$R = \frac{|J_{lewat}|}{|J_{masuk}|} \quad (19)$$

Bound State ($E < 0$)

The potential Schrödinger equation of the delta function in the bound state becomes:

$$\frac{d^2\psi}{dx^2} = -\frac{2m}{\hbar^2} E\psi = \kappa^2\psi \quad (20)$$

The wave function in the bound state or $E < 0$ for the delta function potential is:

$$\Psi_1(x, t) = Ae^{-(\kappa x + i\omega t)} + Be^{(\kappa x - i\omega t)}, \text{ for } (x < 0) \quad (21)$$

$$\Psi_2(x, t) = Fe^{-(\kappa x + i\omega t)} + Ge^{(\kappa x - i\omega t)}, \text{ for } (x > 0) \quad (22)$$

G becomes worth zero. Until the equations (21) and (22) become as follows :

$$\Psi_1(x, t) = Be^{(\kappa x - i\omega t)}, \text{ for } (x < 0) \quad (23)$$

$$\Psi_2(x, t) = Fe^{-(\kappa x + i\omega t)}, \text{ for } (x > 0) \quad (24)$$

Equations (23) and (24) representing the bound state of the delta function ($E < 0$) can be described as figure 2 below:

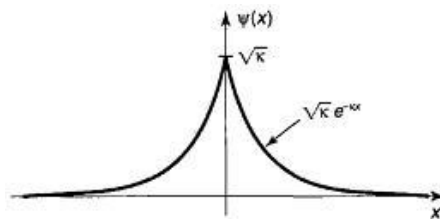


Figure 2. Bound state ($E < 0$) on the delta function (Griffits, 2005:72)

Based on these conditions obtained $F = B$, so that:

$$\Psi(x, t) = \begin{cases} Be^{(\kappa x - i\omega t)} & \text{untuk } (x < 0) \\ Be^{-(\kappa x + i\omega t)} & \text{untuk } (x > 0) \end{cases} \quad (25)$$

$$\kappa = \frac{\sqrt{-2mE}}{\hbar} \quad (26)$$

Therefore, normalizations of equations (23) and (24) to obtain the constants F and B byn give a limit $-\infty$ up to ∞ . The normalization formula can be written as follows:

$$\int_{-\infty}^{\infty} |\Psi(x, t)|^2 dx = 1 \quad (27)$$

Substitute equations (23) and (24) into the normalized formula for equation (27), so that it becomes:

$$\int_{-\infty}^0 (Be^{(\kappa x - i\omega t)})(Be^{(\kappa x + i\omega t)})dx + \int_0^{\infty} (Fe^{-(\kappa x + i\omega t)})(Fe^{-(\kappa x - i\omega t)})dx = 1 \quad (28)$$

So that the value of the constant F is obtained, namely:

$$F = \sqrt{\kappa} \quad (29)$$

Substituting the value of the constant B into the potential wave equation of the delta state function is bound to equations (23) and (24), so it can be written as follows:

$$\Psi_1(x, t) = B e^{(\kappa x - i\omega t)} = \sqrt{\kappa} e^{(\kappa x - i\omega t)} \quad (30)$$

$$\Psi_2(x, t) = F e^{-(\kappa x + i\omega t)} = \sqrt{\kappa} e^{-(\kappa x + i\omega t)} \quad (31)$$

The regularization phase (θ_1) value can be calculated by substituting the position-dependent wave function ψ_1 in equation (30) to equation (10) and θ_2 can be calculated by substituting the position-dependent wave function ψ_2 in equation (31) to equation (10). (θ_1) ψ_1 θ_2 ψ_2

$$\psi_1 = \sqrt{\kappa} e^{(\kappa x)} \quad (32)$$

$$\psi_2 = \sqrt{\kappa} e^{-(\kappa x)} \quad (33)$$

$$\theta_1 = \frac{A_1}{-2\kappa^2} e^{-2\kappa x} \quad (34)$$

Equation (34) can be described in grafik form with input as shown 3 below:

```
κ = 1; A1 = 1;
Plot[ $\frac{A_1}{-2\kappa^2} e^{-2\kappa x}$ , {x, -3, 3}, AxesLabel -> {x,  $\theta_1$ },
LabelStyle -> Directive[12, Black,
FontFamily -> "Times New Roman"]]
```

Figure 3 Input equation (34) for the graph figure 4

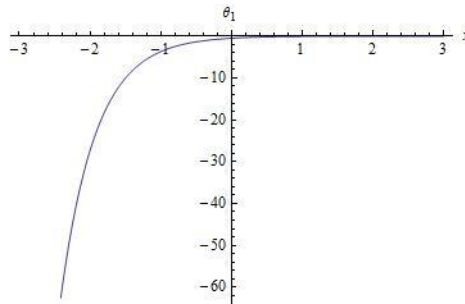


Figure 4 Regularization Phase graph at E < 0 state with ($x < 0$)

Figure 4 above shows that when $x = -1$ m, $\theta_1 = -4$ and when x is positive θ_1 it gets closer to zero. K ethics value x is negative then the value of the regularization phase is negative too, with the greater the value of x the greater the value of the regularization phase. cut the x -axis. Value A_1 is a constant so it is assumed with 1.

$$\theta_2 = \frac{A_1}{2\kappa^2} e^{2\kappa x} \quad (35)$$

Equation (35) can be described in graphic form with inputs such as figure 5 as follows:

```
κ = 1; A1 = 1;
Plot[ $\frac{A_1}{2\kappa^2} e^{2\kappa x}$ , {x, -3, 3}, AxesLabel → {x, θ2},
LabelStyle → Directive[12, Black,
FontFamily → "Times New Roman"]]
```

Figure 5 Input equation (35) for the graph figure 6

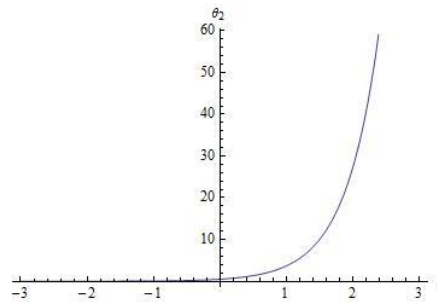


Figure 6 Regularization Phase graph at state $E < 0$ with $(x > 0)$

Figure 6 above shows that when $x = 1$ m, $\theta_2 = 4$ and x is negative the value θ_2 gets closer to zero. κx value is directly proportional to the value of the regularization phase, the greater the value of x , the greater the value of the regularization phase. The regularization phase will be worth infinitely and worth $x \rightarrow +\infty$ towards zero when $x \rightarrow -\infty$. Figure 6 above is an exponential graph.

Based on the regularization phase value obtained, the adiabatic wave function is obtained through substituting the regularization phase value in equations (34) and (35) to equation (6) and can be written as follows:

$$\Psi_1^{(reg)}(x, R(t)) = \sqrt{\kappa} e^{(\kappa x)} e^{-(i/\hbar) \int_0^t E_n(R(t)) dt} e^{i\epsilon \frac{A_1}{-2\kappa^2} e^{-2\kappa x}} \Psi_1^{(reg)}(x, R(t)) = \sqrt{\kappa} e^{(\kappa x)} e^{-(i/\hbar) \int_0^t E_n(R(t)) dt} e^{i\epsilon \frac{A_1}{-2\kappa^2} e^{-2\kappa x}} \quad (36)$$

$$\Psi_2^{(reg)}(x, R(t)) = \sqrt{\kappa} e^{(-\kappa x)} e^{-(i/\hbar) \int_0^t E_n(R(t)) dt} e^{i\epsilon \frac{A_1}{2\kappa^2} e^{2\kappa x}} \quad (37)$$

$$\Psi_2^{(reg)}(x, R(t)) = \sqrt{\kappa} e^{(-\kappa x)} e^{-(i/\hbar) \int_0^t E_n(R(t)) dt} e^{i\epsilon \frac{A_1}{2\kappa^2} e^{2\kappa x}}$$

The equation above can be seen in graphic form by calculating the amplitude value of each wave, with the following formula:

$$|\Psi_1^{(reg)}(x, R(t))|^2 = (\kappa e^{2\kappa x}) \quad (38)$$

Until when depicted in graphic form with inputs such as the following 77 pictures :

```
κ = 1;
Plot[ $\kappa e^{2\kappa x}$ , {x, -3, 0},
AxesLabel → {x,  $|\Psi_1|^2(x, R[t])$ },
LabelStyle → Directive[12, Black,
FontFamily → "Times New Roman"]]
```

Figure 7 Input wave amplitude (equation 38) for the graph in figure 8

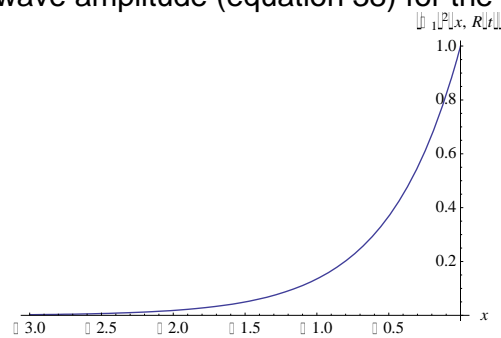
Figure 8. Amplitude graph for $x \leq 0$ in case $E < 0$

Figure 8 above is illustrated with the value $\kappa = 1$, and the value x from -3 to 0 . From the graph above it can be seen that when $x = 0$ the wave function is equal to κ . The smaller the value of x , the wave function is closer to 0 , when x is equal to $-\infty$ the wave function is 0 . The function graph above is an uphill exponential function graph that has the characteristics of never intersecting the x -axis.

The amplitude graph for the regularized wave function at $x > 0$ bound state is as follows:

$$|\Psi_2^{(reg)}(x, R(t))|^2 = (\kappa e^{-2\kappa x}) \quad (39)$$

Equation (39) can be described in graphic form with inputs such as figure 9 below:

```
κ = 1;
Plot[κ e-2κx, {x, 0, 3},
  AxesLabel → {x, |Ψ₁|²[x, R[t]]},
  LabelStyle → Directive[12, Black,
    FontFamily → "Times New Roman"]]
```

Figure 9 Input wave amplitude (equation 39) for the graph in figure 10

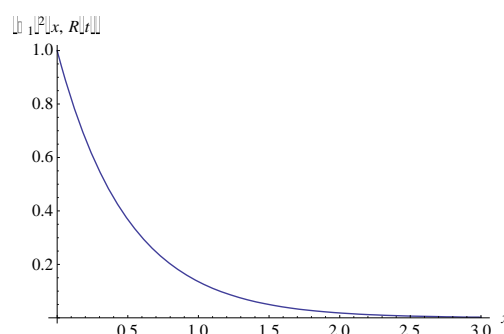
Figure 10. Amplitude graph for $x > 0$ the case $E < 0$

Figure 10 above is illustrated with the value of $\kappa = 1 \text{ m}^{-1}$ and x value from 0 to 3 m . From the graph above it can be seen that when $x = 0 \text{ m}$ the wave function is equal to κ . The wave function gets smaller the smaller the x gets, when x equals $+\infty$ the wave function is 0 . The function graph above is a graph of a descending exponential function that never intersects the x -axis.

Additional potentials can be calculated (\tilde{V}) by substituting position-dependent wave functions ψ_1 and ψ_2 into equation (12). As shown in equation (12), if the wave function is real, the additional potential (\tilde{V}) is zero. So it is written in the equation to be: (\tilde{V})

$$\tilde{V}_1 = 0 \quad (40)$$

$$\tilde{V}_2 = 0 \quad (41)$$

In the bound state $E < 0$, there are only two currents, namely the reflected current (J_{pantul}) and the passing current (J_{lewat}). $E < 0(J_{pantul})(J_{lewat})$

$$\Psi^{(reg)}(x, R(t))_{pantul} = B e^{(\kappa x - i\omega t)} e^{i\epsilon\theta_1(x,t)} \quad (42)$$

$$\Psi^{(reg)}(x, R(t))_{lewat} = F e^{-(\kappa x + i\omega t)} e^{i\epsilon\theta_2(x,t)} \quad (43)$$

The density of the reflected current can be calculated using equation (16) so that: The derivative θ_1 can be calculated so as to produce:

$$\frac{d\theta_1}{dx} = \frac{d \frac{A_1}{-2\kappa^2} e^{-2\kappa x}}{dx} = \frac{A_1}{\kappa} e^{-2\kappa x} \quad (44)$$

The derivative $\Psi^{(reg)}(x, R(t))_{pantul}$ can be calculated so as to produce:

$$\frac{d\Psi^{(reg)}(x, R(t))_{pantul}}{dx} = B \left(\kappa + i\epsilon \frac{A_1}{\kappa} e^{-2\kappa x} \right) e^{(\kappa x - i\omega t)} e^{i\epsilon\theta_1(x,t)} \quad (45)$$

The derivative $\Psi^{(reg)*}(x, R(t))_{pantul}$ can be calculated so as to produce:

$$\frac{d\Psi^{(reg)*}(x, R(t))_{pantul}}{dx} = B \left(\kappa + i\epsilon \frac{A_1}{\kappa} e^{-2\kappa x} \right) e^{(\kappa x - i\omega t)} e^{i\epsilon\theta_1(x,t)} \quad (46)$$

Substituting the derivative products in equations (44), (45), and (46) into equation (16) so that J_{pantul} the value is as follows:

$$J_{pantul} = \frac{\hbar}{m} \left(|B|^2 \left(\epsilon \frac{A_1}{\kappa} e^{-2\kappa x} \right) \right) \quad (47)$$

Equation (47) can be depicted in graphic form with inputs such as figure 11 below:

```
κ = 1; A1 = 1; ħ = 1.05 × 10-34; m = 1; B = 1; ε = 1;
Plot[ $\frac{\hbar}{m} B^2 \left( \epsilon \frac{A_1}{\kappa} e^{-2\kappa x} \right)$ , {x, -3, 3}, AxesLabel → {x, Jpantul},
LabelStyle → Directive[12, Black,
FontFamily → "Times New Roman"]]
```

Figure 11 Input equation (47) for the graph in figure 12

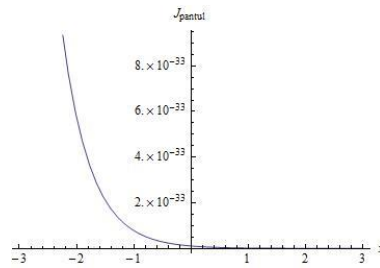


Figure 12 Graph of Bounce Current Meeting in case $E < 0$

Figure 12 above shows that when the density value of the reflected current goes towards zero when the $x \rightarrow +\infty$ current density value goes to infinity. $x \rightarrow -\infty$ then the density value of the reflected current is getting closer to zero. When $x = -1$ m the bounce current density is 0.5×10^{-33} A/m², and when x is positive the bounce current density is close to zero. The density value of the reflected current is inversely proportional to the value of x . Figure 2 is a graph of the descending exponential function.

The density of the current can be calculated using equation (17) so that :
The derivative $\Psi^{(reg)}(x, R(t))_{lewat}$ can be calculated so as to produce:

$$\frac{d\Psi^{(reg)}(x, R(t))_{lewat}}{dx} = F \left(-\kappa + i\varepsilon \frac{A_1}{\kappa} e^{2\kappa x} \right) e^{-(\kappa x + i\omega t)} e^{i\varepsilon\theta_2(x, t)} \quad (48)$$

The derivative $\Psi^{(reg)*}(x, R(t))_{lewat}$ can be calculated so as to produce:

$$\frac{d\Psi^{(reg)*}(x, R(t))_{lewat}}{dx} = F \left(\kappa - i\varepsilon \frac{A_1}{\kappa} e^{2\kappa x} \right) e^{(\kappa x + i\omega t)} e^{-i\varepsilon\theta_2(x, t)} \quad (49)$$

The derivative θ_2 can be calculated so as to produce:

$$\frac{d\theta_2}{dx} = \frac{d\frac{A_1}{2\kappa^2} e^{2\kappa x}}{dx} = \frac{A_1}{\kappa} e^{2\kappa x} \quad (50)$$

Substitution of the derivative results in equations (48), (49), and (50) to equation (16) so that the value is as follows: J_{lewat}

$$J_{lewat} = \frac{\hbar}{m} \left(|F|^2 \left(i\kappa + \varepsilon \frac{A_1}{\kappa} e^{2\kappa x} \right) \right) \quad (51)$$

Equation (51) can be described in graphic form with inputs such as figure 13 below:

```

κ = 1; A1 = 1; ε = 1; F = 1; ħ = 1.05 × 10-34; m = 1;
y = ħ/m F2 (i κ + ε A1/κ e2κx);
Plot[Abs[y], {x, -3, 3}, AxesLabel -> {x, Jlewat},
LabelStyle -> Directive[12, Black,
FontFamily -> "Times New Roman"]]

```

Figure 13 Input equation (51) for the graph in figure 14

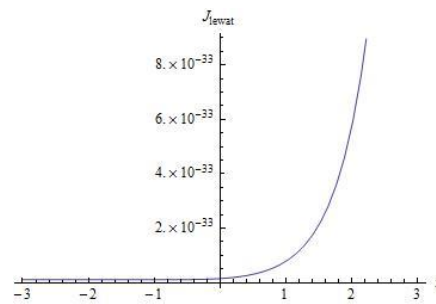


Figure 14 Graph of Passing Current Meeting in case $E < 0$

Figure 14 shows that the density of the current is directly proportional to x , the density of the current increases with the increase of x . When $x = 1$ m of current density is 0.5×10^{-33} A/m² and when x is negative the current density is close to zero where x to the density of the current through is infinite. $x \rightarrow +\infty$ The chart above is an uphill exponential graph.

Scatter State ($E > 0$)

In the scattering state, the Schrödinger equation can be written as follows:

$$\frac{d^2\psi}{dx^2} = -\frac{2m}{\hbar^2} E\psi = -k^2\psi \quad (52)$$

The wave function in the bound state or $E > 0$ for the delta function potential is:

$$\Psi_1(x, t) = A e^{i(kx - \omega t)} + B e^{-i(kx + \omega t)} \text{ for } (x < 0) \quad (53)$$

$$\Psi_2(x, t) = F e^{i(kx - \omega t)} + G e^{-i(kx + \omega t)} \text{ for } (x > 0) \quad (54)$$

Since G is 0, the equation (54) becomes:

$$\Psi_2(x, t) = F e^{i(kx - \omega t)} \text{ for } (x > 0) \quad (55)$$

$$k = \frac{\sqrt{2mE}}{\hbar} \quad (56)$$

Equations (53) and (55) can be described in graphic form as shown 15 below :

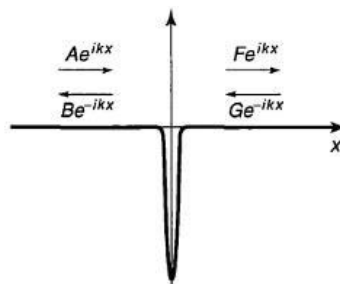


Figure 15 Scattering state ($E > 0$) on delta function potential (Griffits, 2005:72)

By using the properties of continuity $\Psi_1(x, t)$ and $\Psi_2(x, t)$ at the moment $x = 0$ $\Psi_1(x, t) = \Psi_2(x, t)$ at $x = 0$. So it can be written as follows:

$$(A + B) = (F + G) \quad (57)$$

The derivative of $\Psi_1(x, t)$ and $\Psi_2(x, t)$ at the time of $x = 0$ is: $\Psi_1(x, t)\Psi_2(x, t)$

$$\frac{\partial}{\partial x} \Psi_1(x, t) = \frac{\partial}{\partial x} \Psi_2(x, t) \quad (58)$$

$$\Delta \frac{\partial \Psi}{\partial x} = ik(F - G - A + B) \quad (59)$$

By looking at the equation $\Delta \left(\frac{\partial \Psi}{\partial x} \right) = -\frac{2m\alpha}{\hbar^2} \Psi(0)$. Then the above equation can be changed to:

$$ik(F - G - A + B) = -\frac{2m\alpha}{\hbar^2} (A + B) \quad (60)$$

$$F - G = A \left(\frac{2im\alpha}{\hbar^2 k} + 1 \right) - B \left(\frac{-2im\alpha}{\hbar^2 k} + 1 \right) \text{ with } \beta = \frac{m\alpha}{\hbar^2 k} \quad (61)$$

$$F - G = A(1 + 2i\beta) - B(1 - 2i\beta) \quad (62)$$

To find the value of B Substitution of equation (62) to equation (57)

$$B = A \frac{(i\beta)}{(1-i\beta)} \quad (63)$$

$$F = A \left(\frac{1}{(1-i\beta)} \right) \quad (64)$$

Evidenced by the normalization of wave functions in equations (53) and (54) by being limited from $-\infty$ to ∞ those that produce infinite values.

$$\int_{-\infty}^{\infty} |\Psi(x, t)|^2 dx = 1 \quad (65)$$

$$\int_{-\infty}^0 |\Psi_1(x, t)|^2 dx + \int_0^{\infty} |\Psi_2(x, t)|^2 dx = 1 \quad (66)$$

$$\int_0^{\infty} (\Psi_2(x, t))(\Psi_2(x, t))^* dx = 1$$

$$\int_{-\infty}^0 (\Psi_1(x, t))(\Psi_1(x, t))^* dx + \int_0^{\infty} (\Psi_2(x, t))(\Psi_2(x, t))^* dx = 1 \quad (67 \& 68)$$

$$\int_{-\infty}^0 (Ae^{i(kx-\omega t)} + Be^{-i(kx+\omega t)})(Ae^{-i(kx-\omega t)} + Be^{i(kx+\omega t)})dx + \int_0^{\infty} (Fe^{i(kx-\omega t)})(Fe^{-i(kx-\omega t)})dx = 1$$

Substitute equations (63) and (64) to equations (53) and (54) so that a wave function is obtained in the scattering state, which is as follows:

$$\Psi_1(x, t) = A e^{i(kx-\omega t)} + A \frac{(i\beta)}{(1-i\beta)} e^{-i(kx+\omega t)} \quad (69)$$

$$\Psi_2(x, t) = A \left(\frac{1}{(1-i\beta)} \right) e^{i(kx-\omega t)} \quad (70)$$

The regularization phase (θ_1) value can be calculated by substituting the position-dependent wave function ψ_1 in equation (69) to equation (11) and θ_2 can be calculated by substituting the position-dependent wave function ψ_2 in equation (31) to equation (11). $(\theta_1)\psi_1 \theta_2\psi_2$

$$\psi_1 = A e^{i(kx)} + A \frac{(i\beta)}{(1-i\beta)} e^{-i(kx)} \quad (71)$$

$$\psi_2 = A \left(\frac{1}{(1-i\beta)} \right) e^{i(kx)} \quad (72)$$

$$\theta_1 = \frac{A_1 x}{A^2 \left(1 + \frac{(-i\beta)}{(1+i\beta)} e^{2ikx} + \frac{(i\beta)}{(1-i\beta)} e^{-2ikx} + \frac{(\beta^2)}{(1+\beta^2)} \right)} \quad (73)$$

Equation (73) can be described in graphic form with inputs such as figure 16 below:

```

A = 1; k = 1; A1 = 1; β = 1;
Plot[  $\frac{A_1 x}{A^2 \left( 1 + \left( \frac{-i\beta}{1+i\beta} \right) e^{2ikx} + \frac{i\beta}{1-i\beta} e^{-2ikx} + \frac{\beta^2}{1+\beta^2} \right)}$  ,
{x, -10, 10}, AxesLabel → {x, θ1},
LabelStyle → Directive[12, Black,
FontFamily → "Times New Roman"]]

```

Figure 16 Input equation (73) for the graph in figure 17

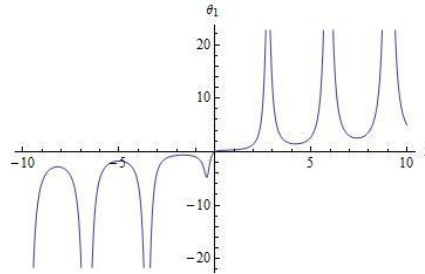


Figure 17 Regularization Phase at E>0 with (x < 0)

Figure 17 shows that the regularization phase hits a satellite dish every 3 m.

$$\theta_2 = \frac{A_2 x (1 + \beta^2)}{A^2} \quad (74)$$

Equation (74) can be described in graphic form with inputs such as figure 18 below:

```

A = 1; A1 = 1; β = 1;
Plot[  $\frac{A_1 x (1 + \beta^2)}{A^2}$  , {x, -3, 3}, AxesLabel → {x, θ2},
LabelStyle → Directive[12, Black,
FontFamily → "Times New Roman"]]

```

Figure 18 Input equation (74) for the graph in figure 19

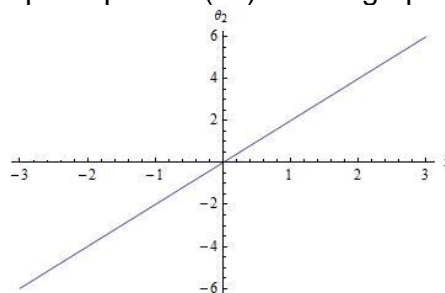


Figure 19 Regularization Phase Graph at E>0 with (x > 0)

Figure 19 above shows that the value of the regularization phase at E>0 is (x > 0) directly proportional to the value of x, the greater the value of x, the greater the regularization phase. The gradient above is a linear graph.

The adiabatic wave function is obtained through substituting the regularization phase value in equations (73) and (74) to equation (5) and can be written as follows:

$$\Psi_1^{(reg)}(x, R(t)) = \left(A e^{i(kx)} + A \frac{(i\beta)}{(1-i\beta)} e^{-i(kx)} \right) e^{-(i/\hbar) \int_0^t E_n(R(t)) dt} e^{i\epsilon \frac{A_1 x}{A^2 \left(1 + \frac{(-i\beta)}{(1+i\beta)} e^{2ikx} + \frac{(i\beta)}{(1-i\beta)} e^{-2ikx} + \frac{(\beta^2)}{(1+\beta^2)} \right)}}$$

$$\Psi_1^{(reg)}(x, R(t)) = \left(A e^{i(kx)} + A \frac{(i\beta)}{(1-i\beta)} e^{-i(kx)} \right) e^{-(i/\hbar) \int_0^t E_n(R(t)) dt} e^{i\epsilon \frac{A_1 x}{A^2 \left(1 + \frac{(-i\beta)}{(1+i\beta)} e^{2ikx} + \frac{(i\beta)}{(1-i\beta)} e^{-2ikx} + \frac{(\beta^2)}{(1+\beta^2)} \right)}}$$

$$\Psi_2^{(reg)}(x, R(t)) = A \left(\frac{1}{(1-i\beta)} \right) e^{i(kx)} e^{-(i/\hbar) \int_0^t E_n(R(t)) dt} e^{i\epsilon \frac{A_2 x(1+\beta^2)}{A^2}}$$

$$\Psi_2^{(reg)}(x, R(t)) = A \left(\frac{1}{(1-i\beta)} \right) e^{i(kx)} e^{-(i/\hbar) \int_0^t E_n(R(t)) dt} e^{i\epsilon \frac{A_2 x(1+\beta^2)}{A^2}}$$

Equation (75) above can be seen in graph form by calculating the amplitude value of each wave, with the following formula:

$$|\Psi_1^{(reg)}(x, R(t))|^2 = A^2 \left(1 + \frac{(-i\beta)}{(1+i\beta)} e^{2ikx} + \frac{(i\beta)}{(1-i\beta)} e^{-2ikx} + \frac{(\beta^2)}{(1+\beta^2)} \right) \quad (77)$$

Equation (77) can be described in graphform with inputs such as figure 2020 below:

```
k = 1; β = 1; A = 1
Plot[A^2 (1 + (-i β)/(1 + i β) e^(2 i k x) + (i β)/(1 - i β) e^(-2 i k x) + β^2/(1 + β^2)),
{x, -5, 5}, AxesLabel -> {x, |Ψ1|2[x, R[t]]},
LabelStyle -> Directive[12, Black,
FontFamily -> "Times New Roman"]]
```

Figure 20 Input wave amplitude (equation 77) for the graph in figure 21

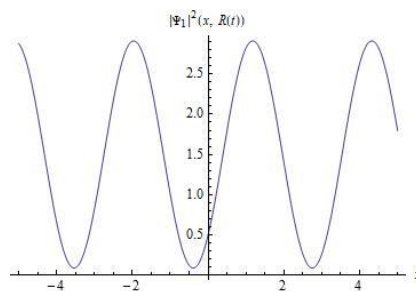


Figure 21. 2-dimensional graph of the amplitude of the wave function of the scattering state ($E > 0$) at $x < 0$ by $k = 1$

Figure 21 above is depicted with values $\beta = 1$, $k = 1 \text{ m}^{-1}$, $\beta = 1A = 1$, and x from -5 to 5 m . When $x = -2 \text{ m}$ the wave reaches the maximum value of 2.9 m and when $x = -3.5 \text{ m}$ the wave reaches the minimum value of 0.1 m . It can be seen that the

gelombang hanya sedikit tetapi panjang gelombang besar. Nilai k berbanding lurus dengan panjang gelombang tetapi berbanding terbalik dengan banyak gelombang.

```
k = 3; β = 1; A = 1
Plot[A^2 (1 +  $\frac{-i\beta}{1+i\beta} e^{2ikx} + \frac{i\beta}{1-i\beta} e^{-2ikx} + \frac{\beta^2}{1+\beta^2}$ ),
{x, -5, 5}, AxesLabel -> {x,  $|\Psi_1|^2[x, R[t]]$ },
LabelStyle -> Directive[12, Black,
FontFamily -> "Times New Roman"]]
```

Figure 22 Input wave amplitude (equation 77) for the graph in figure 23

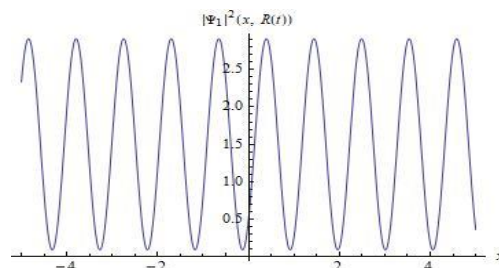


Figure 23. 2-dimensional graph of the amplitude of the wave function of the scattering state ($E > 0$) at $x < 0$ with $k = 3$

Figure 23 above is depicted with values $\beta = 1$, $k = 3 \text{ m}^{-1}$, $\beta = 1$, $A = 1$, and x from -5 m to 5 m . You can see more waves than figure 19. The higher the k , the more waves formed. The lower the k , the fewer waves formed. Many waves are formed inversely proportional to k .

Equation (77) can be depicted in the form of a 3-dimensional graph with input such as figure 24 below:

```
β = 1; A = 1;
Plot3D[A^2 (1 +  $\frac{-i\beta}{1+i\beta} e^{2ikx} + \frac{i\beta}{1-i\beta} e^{-2ikx} + \frac{\beta^2}{1+\beta^2}$ ),
{x, -5, 5}, {k, -1, 1},
AxesLabel -> {x, k,  $|\Psi_1|^2[x, R[t]]$ },
LabelStyle -> Directive[12, Black,
FontFamily -> "Times New Roman"]]
```

Figure 24 Input equation (77) for the graph in figure 25

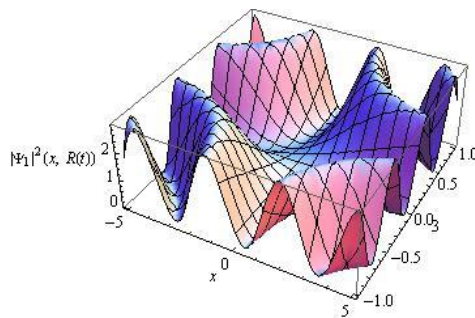


Figure 25 3-dimensional graph of the amplitude wave function to the scattering form ($E > 0$) at $x < 0$

Figure 25 above is illustrated with $\beta = 1$, $A = 1$, x from -5 to 5β , and k from -1 to 1 .

The amplitude graph for the regularized wave function at $x_0 \geq \text{scattering state}$ is as follows:

$$|\Psi_2^{(reg)}(x, R(t))|^2 = A^2 \left(\frac{1}{1+\beta^2} \right) \quad (78)$$

up to the equation (78) when depicted in the form of a 2-dimensional graphic with inputs such as the following picture 26 :

```
 $\beta = 1;$ 
Plot[ $A^2 \left( \frac{1}{1+\beta^2} \right)$ , {A, -5, 5},
AxesLabel → {x,  $|\Psi_1|^2[x, R[t]]$ },
LabelStyle → Directive[12, Black,
FontFamily → "Times New Roman"]]
```

Figure 24 Input amplitude of the wave (perequation 78) graph in figure 27

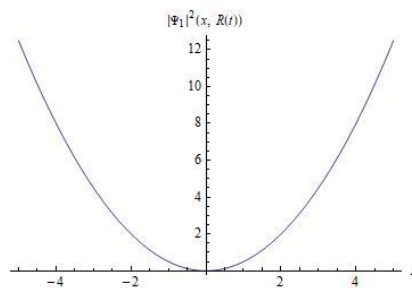


Figure 25. 2-dimensional graph of the amplitudo of the wave function of the scattering state ($E > 0$) at $x > 0$

Figure 27 above is illustrated with the value $\beta = 1$, $\beta = 1$ and the value A from -5 m to 5 m. It can be seen that at $A = -5$ and 5 the wave function is of enormous value even towards infinity. Whereas when A approaches 0 the wave function goes to zero. The graph above is a parabolic graph.

Equation (78) when depicted in the form of a 3-dimensional graph with input can be seen as figure 28 below:

```
 $\kappa = 1; A_1 = 1;$ 
Plot[ $\frac{A_1}{2\kappa^2} e^{2\kappa x}$ , {x, -3, 3}, AxesLabel → {x,  $\theta_2$ },
LabelStyle → Directive[12, Black,
FontFamily → "Times New Roman"]]
```

Figure 26 Input equation (78) for the graph in figure 29

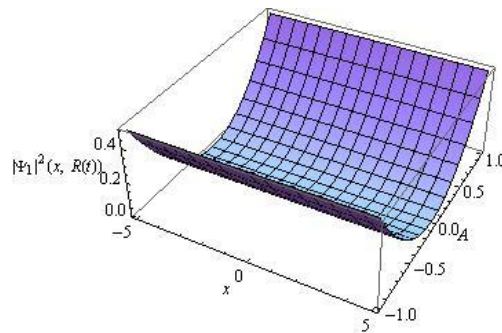


Figure 27. 3-dimensional graph of the amplitude of the scattering state wave function ($E > 0$) at $x > 0$ when x and A are varied

Figure 29 above is illustrated with $\beta = 1$, x from -5 to 5 $\beta = 1\text{m}$, and A from -1 to 1 . It can be seen that when $A = -1$ and 1 the wave function goes to infinity, while when A approaches zero the wave function goes to zero.

Equation (78) when depicted in the form of a 3-dimensional graph with x and t varied with input can be seen as figure 30 below:

```
A = 1
Plot3D[A^2 (1/(1 + β^2)), {x, -5, 5}, {t, -1, 1},
  AxesLabel -> {x, t, |Ψ₁|²[x, R[t]]},
  LabelStyle -> Directive[12, Black,
    FontFamily -> "Times New Roman"]]
```

Figure 30 Input equation (78) for the graph in figure 31

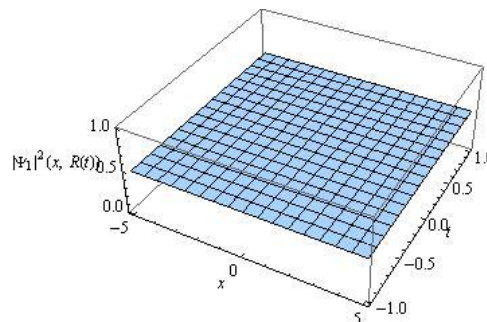


Figure 31 Graphic amplitude wave function on $x \geq 0$ scattering state

Figure 31 above is illustrated with $\beta = 1$, $k = 1 \text{ m}^{-1}$, $\beta \omega = 1 \text{ rad/s}$, $A = 1$, x from -5 to 5 m , and $t\omega = 1$ from -1 to 1 . The wave function is constant even if the variables x and t are changed.

Additional potentials can be calculated (\tilde{V}) by substituting position-dependent wave functions in equation (71) and in equation (72) to equation (13). The wave function depends on position $\psi_1\psi_2\psi_1$ and ψ_2 is imaginary so it is written in the equation to be:

$$\frac{d\psi_1}{dx} = \left(Aik e^{i(kx)} - A \frac{(i\beta)}{(1-i\beta)} ike^{-i(kx)} \right) \quad (79)$$

$$\frac{d\theta_1}{dx} = \frac{d}{dx} \frac{A_1 x}{A^2 \left(1 + \frac{(-i\beta)}{(1+i\beta)} e^{2ikx} + \frac{(i\beta)}{(1-i\beta)} e^{-2ikx} + \frac{(\beta^2)}{(1+\beta^2)} \right)} \quad (80)$$

Substitute equations (79) and (80) to equation (13) so that it becomes

$$\tilde{V}_1 = -\frac{\hbar^2}{m_0} \left(\frac{A i k e^{i(kx)} - A \frac{(i\beta)}{(1-i\beta)} i k e^{-i(kx)}}{A e^{i(kx)} + A \frac{(i\beta)}{(1-i\beta)} e^{-i(kx)}} \right) \alpha \quad (81)$$

Equation (81) can be described in graphic form with inputs such as the following figure :

```
A = 1; k = 1; β = 1; α = 1 ħ = 1.05 × 10-34; m0 = 1;
y = -ħ2 / m0 ( (A i k ei k x - A (iβ / (1-iβ)) i k e-i k x) / (A ei k x + A (iβ / (1-iβ)) e-i k x) ) α;
Plot[Abs[y], {x, -5, 5}, AxesLabel → {x, V̂1},
LabelStyle → Directive[12, Black,
FontFamily → "Times New Roman"]]
```

Figure 32 Input equation (81) for the graph in figure 33

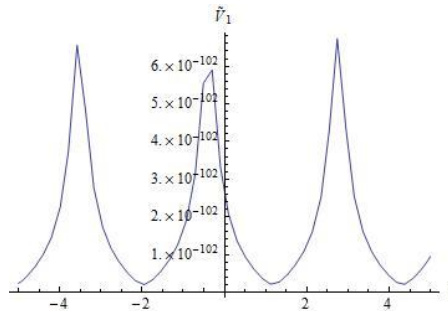


Figure 33 Additional potential graph on at E>0 with (x < 0)

Figure 33 above shows that additional potential forms at E>0 by (x < 0) forming a parabola. When x = 3 m, the potential is 6 × 10⁻¹⁰² Volts.

The additional potential \tilde{V}_2 is lowered in the regularization phase and the additional potential so that it becomes: \tilde{V}_2

$$\frac{d\psi_2}{dx} = i k A \left(\frac{1}{(1-i\beta)} \right) e^{i(kx)} \quad (82)$$

$$\frac{d\theta_2}{dx} = \frac{A_2(1+\beta^2)}{A^2} \quad (83)$$

Substituting equations (82) and (83) for equation (13) to find \tilde{V}_2 so that it can be written as

$$\tilde{V}_2 = -\frac{\hbar^2}{m_0} i k \frac{A_2(1+\beta^2)}{A^2} \quad (84)$$

Equation (84) can be described in the form of a graph with inputs such as figure 34 below:

```

A = 1; ħ = 1.05 × 10-34; m0 = 1; β = 1; A2 = 1;
y =  $\frac{-\hbar^2}{m_0} i k \frac{A_2 (1 + \beta^2)}{A^2}$ 
Plot[Abs[y], {k, -3, 3}, AxesLabel → {k,  $\tilde{v}_2$ },
LabelStyle → Directive[12, Black,
FontFamily → "Times New Roman"]]

```

Figure 34 Input equation (84) for grafik in figure 35

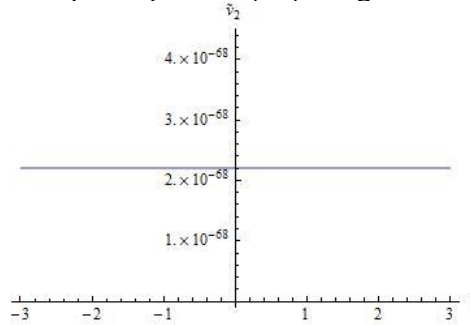
Figure 35 Additional potential graph at $E > 0$ with $x > 0$

Figure 35 above shows that the additional potential value is constant with a value of 2.2×10^{-68} Volts, does not change even though the k value is changed.

In the scattering state or $E > 0$ there are three currents, namely inflow, passing current and reflecting current.

$$\Psi^{(reg)}(x, R(t))_{masuk} = A e^{i(kx - \omega t)} e^{i\epsilon\theta_1(x,t)} \quad (85)$$

$$\Psi^{(reg)}(x, R(t))_{pantul} = B e^{-i(kx + \omega t)} e^{i\epsilon\theta_1(x,t)} \quad (86)$$

$$\Psi^{(reg)}(x, R(t))_{lewat} = F e^{i(kx - i\omega t)} e^{i\epsilon\theta_2(x,t)} \quad (87)$$

The density of the inflow can be found using equation (15).

$$\begin{aligned} \frac{d\Psi^{(reg)}(x, R(t))_{masuk}}{dx} &= \\ A(ik + i\epsilon\alpha) e^{i(kx - \omega t)} e^{i\epsilon\theta_1(x,t)} &= \\ \frac{d\Psi^{(reg)}(x, R(t))_{masuk}}{dx} &= \\ A(ik + i\epsilon\alpha) e^{i(kx - \omega t)} e^{i\epsilon\theta_1(x,t)} &= \end{aligned} \quad (88)$$

$$\begin{aligned} \frac{d\Psi^{(reg)*}(x, R(t))_{masuk}}{dx} &= \\ A(-ik - i\epsilon\alpha) e^{-i(kx - \omega t)} e^{-i\epsilon\theta_1(x,t)} &= \\ \frac{d\Psi^{(reg)*}(x, R(t))_{masuk}}{dx} &= A(-ik - i\epsilon\alpha) e^{-i(kx - \omega t)} e^{-i\epsilon\theta_1(x,t)} \end{aligned} \quad (89)$$

Substitution of the derivative results in equation (88) and equation (89) to equation (15) so that it J_{masuk} gets: J_{masuk}

$$J_{masuk} = \frac{\hbar}{m} |A|^2 (k + \epsilon\alpha) \quad (90)$$

Equation (90) can be described in graphic form with inputs as shown in the following figure 36

```
A = 1; ħ = 1.05 × 10-34; m = 1; ε = 1; α = 1;
Plot[ $\frac{\hbar}{m}$  Abs[A]2 (k + ε α), {k, -2, 2},
AxesLabel → {k, Jmasuk},
LabelStyle → Directive[12, Black,
FontFamily → "Times New Roman"]]
Clear[k]
```

Figure 36 Input equation (90) for the graph figure 37

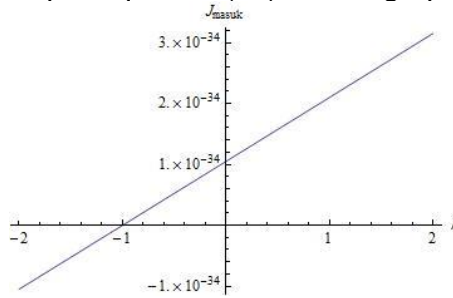


Figure 37 Inflow density graph at (E>0)

Figure 37 above shows that the inflow density graph includes a linear function graph, where the value of k is directly proportional to the density of the inflow, the greater the value of k , the greater the value of the current density. When $k = -1 \text{ m}^{-1}$ the inrush current density value is 0, and when $k = 0 \text{ m}^{-1}$ the current density value is $1 \times 10^{-34} \text{ A/m}^2$.

The density of the reflected current can be calculated as follows:

$$\begin{aligned} \frac{d\Psi^{(reg)*}(x, R(t))_{pantul}}{dx} &= B(ik - i\varepsilon\alpha)e^{i(kx+\omega t)}e^{-i\varepsilon\theta_1(x,t)} \\ \frac{d\Psi^{(reg)*}(x, R(t))_{pantul}}{dx} &= \\ B(ik - i\varepsilon\alpha)e^{i(kx+\omega t)}e^{-i\varepsilon\theta_1(x,t)} \\ \frac{d\Psi^{(reg)*}(x, R(t))_{pantul}}{dx} &= \\ B(ik - i\varepsilon\alpha)e^{i(kx+\omega t)}e^{-i\varepsilon\theta_1(x,t)} & \quad (91) \end{aligned}$$

$$\begin{aligned} \frac{d\Psi^{(reg)}(x, R(t))_{pantul}}{dx} &= \\ B(-ik + i\varepsilon\alpha)e^{-i(kx+\omega t)}e^{i\varepsilon\theta_1(x,t)} \\ \frac{d\Psi^{(reg)}(x, R(t))_{pantul}}{dx} &= B(-ik + i\varepsilon\alpha)e^{-i(kx+\omega t)}e^{i\varepsilon\theta_1(x,t)} & \quad (92) \end{aligned}$$

Substitution of equations (91) and (92) to equations (16) until J_{pantul} they become: J_{pantul}

$$J_{pantul} = \frac{\hbar}{m} |B|^2 (-k + \varepsilon\alpha) \quad (93)$$

Equation (93) can be described in graphic form with inputs such as figure 38 below:

```
B = 1; ħ = 1.05 × 10-34; m = 1; ε = 1; α = 1;
Plot[ $\frac{\hbar}{m}$  Abs[B]2 (-k + ε α), {k, -2, 2},
  AxesLabel → {k, Jpantul},
  LabelStyle → Directive[12, Black,
    FontFamily → "Times New Roman"]]
Clear[k]
```

Figure 38 Inputinput (93) for graphic figure 39

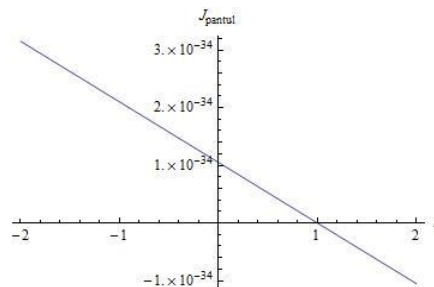


Figure 39 Bounce current density graph for (E>0)

Figure 39 above includes a graph of a linear function where the value of the density of the reflected current is inversely proportional to the value of k, the greater the k the value of the current density the smaller. At the time $k = 1 \text{ m } 1$ the current density is 0, and at the time of the current density is $1 \times 10^{-34} \text{ A/m}^2$, k is 0.

The current pass density can be calculated as follows:

$$\begin{aligned} \frac{dF e^{-i(kx-i\omega t)} e^{-i\varepsilon\theta_2(x,t)}}{dx} &= F \left(-ik - i\varepsilon \frac{A_2(1+\beta^2)}{A^2} \right) e^{-i(kx-i\omega t)} e^{-i\varepsilon\theta_2(x,t)} \\ \frac{dF e^{-i(kx-i\omega t)} e^{-i\varepsilon\theta_2(x,t)}}{dx} &= F \left(-ik - i\varepsilon \frac{A_2(1+\beta^2)}{A^2} \right) e^{-i(kx-i\omega t)} e^{-i\varepsilon\theta_2(x,t)} \\ e^{-i(kx-i\omega t)} e^{-i\varepsilon\theta_2(x,t)} \frac{dF e^{-i(kx-i\omega t)} e^{-i\varepsilon\theta_2(x,t)}}{dx} &= F \left(-ik - i\varepsilon \frac{A_2(1+\beta^2)}{A^2} \right) e^{-i(kx-i\omega t)} e^{-i\varepsilon\theta_2(x,t)} \end{aligned} \quad (94)$$

$$\begin{aligned} \frac{dF e^{i(kx-i\omega t)} e^{i\varepsilon\theta_2(x,t)}}{dx} &= F \left(ik + i\varepsilon \frac{A_2(1+\beta^2)}{A^2} \right) e^{i(kx-i\omega t)} e^{i\varepsilon\theta_2(x,t)} \\ e^{i(kx-i\omega t)} e^{i\varepsilon\theta_2(x,t)} \frac{dF e^{i(kx-i\omega t)} e^{i\varepsilon\theta_2(x,t)}}{dx} &= F \left(ik + i\varepsilon \frac{A_2(1+\beta^2)}{A^2} \right) e^{i(kx-i\omega t)} e^{i\varepsilon\theta_2(x,t)} \end{aligned} \quad (95)$$

Substitution of equations (94) and (95) to equations (17) until J_{lewat} they become:

$$J_{\text{lewat}} = \frac{\hbar}{m} |F|^2 \left(k + \varepsilon \frac{A_2(1+\beta^2)}{A^2} \right) \quad (96)$$

with J_{masuk} is the inrush current density, J_{pantul} is the reflection current density and J_{lewat} is the current passing density. $J_{\text{masuk}} J_{\text{pantul}} J_{\text{lewat}}$

Equation (96) can be described in graphic form with inputs such as the following figure 40:

```
F = 1; ħ = 1.05 × 10-34; m = 1; ε = 1; A = 1; A2 = 1;
β = 1; y =  $\frac{\hbar}{m} F^2 \left( k + \varepsilon \frac{A_2 (1 + \beta^2)}{A^2} \right)$ ;
Plot[Abs[y], {k, -10, 10}, AxesLabel → {k, Jlewat},
LabelStyle → Directive[12, Black,
FontFamily → "Times New Roman"]]
```

Figure 40 Input equation (96) for the graph in figure 41

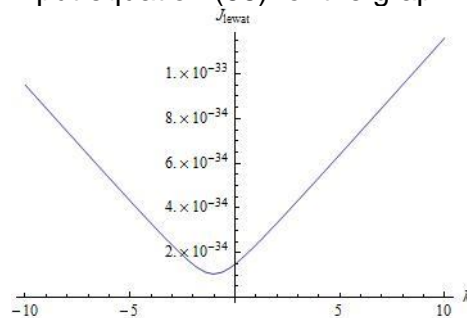


Figure 41 Current meeting for ($E > 0$)

Figure 41 above shows that the minimum current density value passes at $k = -1 \text{ m}^{-1}$ and goes up as the value of k increases.

Conclusion

In this study, regularization phases and additional potentials have been obtained that are able to maintain adiabatic quantum dynamics at the delta function potential. In addition, solutions of wave functions, delta functions, and current density are also obtained. From the results of this study, it was found that the wave function in the state $E < 0$ forms a graph of the exponential function uphill for $x < 0$ and decreased for $x > 0$ where when $x = 0 < m$ the wave function $x > 0$ is equal to κ , while the wave function in the state $E > 0$ forms an amplitude graph with a wavelength directly proportional to the value of k , κ when $x = -2 \text{ m}$ wave reaches a maximum value of 2.9 m and when $x = -3.5 \text{ m}$ wave reaches a minimum value of 0.1 m . The regularization phase at state $E < 0$ forms an exponential graph, and never intersects the x axis where at $x < 0$ when the value of $x = -1 \text{ m}$, $\theta_1 = -4$ and when x positive θ_1 gets closer to zero while $x > 0$ when $x = 1$, $\theta_1 = 4$ and at x negative value θ_2 the value gets closer to $x > 0$ θ_2 zero. In the $E > 0$ state, the regularization phase forms a graph that opens up and down, with a constant increase in the minimum value and a constant decrease in the maximum value for ($x < 0$). The additional potential on the state $E < 0$ is zero. Pexists state $E > 0$ forming a parabola for ($x < 0$) where when $x = 3 \text{ m}$, the potential is $6 \times 10^{-102} \text{ Volts}$ and forms a constant graph for $\times 10^{-102} x > 0$ with a value of $2.2 \times 10^{-68} \text{ Volts}$, and forms a linear graph for ($x > 0$) $\times 10^{-68}$. ($x > 0$) The current density in the state forms a graph of the decreasing exponential function for the bounce current density $E < 0$, where k ethics $x = -1 \text{ m}$ the bounce current density is $0.5 \times 10^{-33} \text{ A/m}^2$, and when x is positive the bounce current density is close to nol. Theexponential density rises to the current density through which $\times 10^{-33}$

when $x = 1 \text{ m}$ The density of the passing current is $0.5 \times 10^{-33} \text{ A/m}^2$, and when x is negative the density of the passing current is close to zero. At state ($E > 0$) the inflow and reflection density form a linear graph. On the graph of the density of the inflow when $k = -1 \text{ m}^{-1}$ the value of the density of the inflow is 0, and when $k = 0 \text{ m}^{-1}$ the value of the density of the current is $1 \times 10^{-34} \text{ A/m}^2$. On the graph of the density of the reflected current when $k = 1$ the current density is 0, and when the current density is $1 \times 10^{-34} \text{ A/m}^2$, k is $0 \times 10^{-34} \text{ m}$. Divide the current density through forming a parabolic graph where the minimum current density value passes at $k = -1 \text{ m}$ and goes up as the value of k increases.

References

- Ainayah, N., Setiawan, I., & Hamdani, D. (2022). *The method for accelerating equilibrium in Brownian motion is perfectly muffled*. xx(xx), 1–11. <https://doi.org/https://dx.doi.org/10.23887/jst-undiksha.v11i1>
- Benggadinda, A., & Setiawan, I. (2021). Fast forward method to accelerate adiabatic quantum dynamics on a single spin. *JST (Journal of Science and Technology)*, 10(2), 274–280. <https://doi.org/10.23887/jstundiksha.v10i2.39876>
- Cari, Suparmi, & Marini, H. (2012). Determination of Energy Spectrum and Morse Potential Wave Function by Centrifugal Correction Using SWKB Method and SUSY Operator. *Indonesian Journal of Applied Physics*(2012), 2(2), 1–12.
- Del Campo, A. (2013). Shortcuts to adiabaticity by counterdiabatic driving. *Physical Review Letters*, 111(10), 1–5. <https://doi.org/10.1103/PhysRevLett.111.100502>
- Dianawati, D. A., Suparmi, A., & Cari, C. (2017). Preface: International Conference on Recent Trends in Physics (ICRTP 2016). *Journal of Physics: Conference Series*, 755(1), 1–8. <https://doi.org/10.1088/1742-6596/755/1/011001>
- Elisa, N., Setiawan, I., & Hamdani, D. (2022). *Propulsion Energy to Accelerate Brownian Motion Equilibrium Partially Muffled (Underdamped)*. XX(xx), 1–13.
- Griffiths, D. J. (2005). *Introduction to Quantum Mechanics Second Edition* (Two). Pearson Prentice Hall.
- Guéry-Odelin, D., Ruschhaupt, A., Kiely, A., Torrontegui, E., Martínez-Garaot, S., & Muga, J. G. (2019). Shortcuts to adiabaticity: Concepts, methods, and applications. *Reviews of Modern Physics*, 91(4), 1–61. <https://doi.org/10.1103/RevModPhys.91.045001>
- Haswati, D., & Nopitasari, D. (2019). *Implementation of Differential Equation Teaching Materials with Guided Discovery Method Assisted by Mathematica Software to Improve Concept Understanding*. 2, 97–102.
- Hutagalung, M., Setiawan, I., & Hamdani, D. (2023). Literature review of adiabatic phase to accelerate adiabatic quantum dynamics in harmonic oscillators. *Indonesian Journal of Applied Physics (IJAP)*, 1–13.

- Khujakulov, A., & Nakamura, K. (2016). Scheme for accelerating quantum tunneling dynamics. *Physical Review A*, 93(2), 1–11. <https://doi.org/10.1103/PhysRevA.93.022101>
- Masuda, S., & Nakamura, K. (2022). *Fast-forward scaling theory Subject Areas* : akamura, K., Khujakulov, A., Avazbaev, S., & Masuda, S. (2017). Fast forward of adiabatic control of tunneling states. *Physical Review A*, 95(6), 1–12. <https://doi.org/10.1103/PhysRevA.95.062108>
- Novita, J. S., Dewi, S. N., Mufdhila, A. R., Amalia, A., Viridi, S., Science, K., Nuclear, F., Mathematics, F., Alam, P., & Bandung, I. T. (2017). *Macro and Micro Conditions with Statistical Physics as the Initial Configuration for Optimization of Congregational Prayer Shaf using Agent Based Modeling*. 189–194.
- Restu, Saputra, M. I., Triyono, A., & Suwaji. (2021). *Research Methods*. Depublish.
- Setiawan, I. (2019). Adiabatic quantum spin dynamics are accelerated in the Landau-Zener model and the Ising model. *Journal of Coil Physics*, 2(1), 57–64. <https://doi.org/10.33369/jkf.2.1.57-64>
- Setiawan, I., Gunara, B. E., Avazbaev, S., & Nakamura, K. (2019). *Fast-forward approach to adiabatic quantum dynamics of regular spin clusters: nature of geometry-dependent driving interactions*. 1–17.
- Setiawan, I., Gunara, B. E., Masuda, S., & Nakamura, K. (2018). *Fast forward of adiabatic spin dynamics of entangled states*. 2, 1–13.
- Setiawan, I., Gunara, B. E., & Nakamura, K. (2019). *Fast forward of adiabatic spin dynamics : An application to quantum annealing model in triangle spin systems*. 0–9. <https://doi.org/10.1088/1742-6596/1245/1/012077>
- Sunaryo, Y. (2020). *Mathematical representation skills through problem-based learning assisted by Wolfram Mathematica software*. 4(1), 85–94.
- Susanti, R. J., Noviani, E., & Fran, F. (2019). Mathematical modeling for electric potential difference equations. *Bimaster : Scientific Bulletin of Mathematics, Statistics and Its Applications*, 8(4), 691–698. <https://doi.org/10.26418/bbimst.v8i4.35881>
- Syaifudin, M., Suparmi, S., & Cari, C. (2015). Solving the Schrödinger equation of noncentral potential hyperbolic scarf plus trigonometric Rosen-Morse using *Spectra: Journal of Physics and ...*, 16(2), 20–24. <http://journal.unj.ac.id/unj/index.php/spektra/article/view/5818>